SSRG International Journal of Electrical and Electronics Engineering
ISSN: 2348 – 8379 /doi:10.14445/23488379/IJEEE-V7I10P104

Volume 7 Issue 10, 22-27, October 2020

Reseach on Solutions to Improve the Quality of Renewable Energy Electrical Power in the Micro Grids with FESS

Dinh Tho Long[#1], Vu Thi To Linh[#2], Tran Duc Chuyen[*3], Hoang Dinh Co[#4]

[*#]*Faculty of Electrical, University of Economics - Technology for Industries, Vietnam*

Abstract

In this paper, the authors present a solution to integrate Flywheel Energy Storage System (FESS) with solar power system working in micro-grid to improve the quality of renewable energy electrical sources supplied to the grid. Since then, research in modeling and simulation on Matlab - Simulink software has shown that the FESS can overcome the energy fluctuations of solar power to provide a less changing energy for the grid. Experimental results with three-phase inverters to show that the structure system control always works well, ensuring the power quality standard IEEE 519.

Keywords: *Renewable energy; Solar Power; Microgrid; FESS.*

INTRODUCTION

Today the exhaustion of natural fossil fuels; Oil, along with the influence of the greenhouse effect leads to an urgent need to build and use renewable energy. Among renewable new energy sources, thanks to the rapid development of power electronics; Solar energy and wind energy are becoming more and more popular, these energy sources have replaced traditional fossil energy sources. This is a suitable choice for many countries around the world, [1] - [4], [11, 12].

One energy storage technology that is attracting great interest is the energy storage flywheel (FESS: flywheel energy storage system) [3], [5]. This storage technology has many advantages over other storage solutions such as high life cycle, large energy storage density, unlimited energy storage capacity, and low operating cost. They are effectively applied to smooth the capacity of renewable energy power systems working in the micro-grid (small and medium-sized power grids; allowing integration into the national grid) while ensuring that guarantee the IEEE 519 power quality standard, [10] - [12].

As in a number of research projects in the country [4] and abroad, [5, 6] have not studied in-depth and are only simulating, have not come to experiment to evaluate the quality. power source for the micro-grid.

This paper proposes a renewable electric energy system, with integrated energy storage flywheel (figure 1). An electric machine integrated in the flywheel can work in generator mode or motor mode to convert energy from mechanical to electric and vice versa to stabilize the capacity of the renewable energy system; FESS integrated solar power is supplied to the microgrid.

II. STORAGE ENERGY IN THE MICROGRIDS AND STABILIZING THE GRID FREQUENCY

A. Overview of electricity in the micro-grid

The block diagram of a renewable energy grid with the participation of an energy storage element is shown in Figure 1:

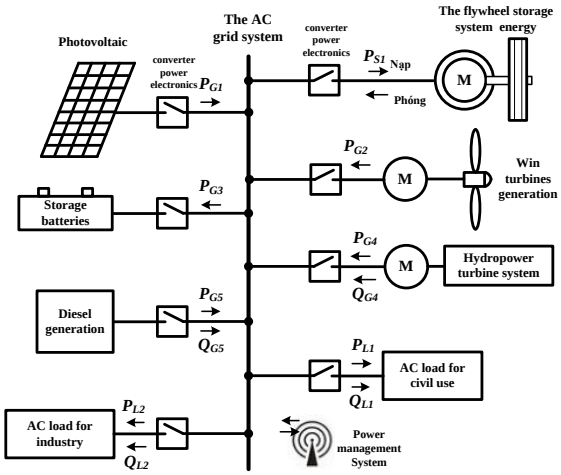

Fig 1: The Microgrid system main components

Energy system is renewable energy sources such as (solar energy, wind turbine, water, energy battery, etc...). The energy collection / generation system is responsible for charging and storing energy when there is an excess and discharge of energy when there are abnormal fluctuations of the grid. This can be done using batteries, batteries, supercapacitors or energy storage flywheels.

Power electronic block is a power electronic converter is connected to the grid flexibly including: Converter DC / AC, AC / DC, etc. For source generator. This mass energy converts the renewable energy into electricity with the right voltage, frequency and phase angle to connect to the micro-grid. For energy storage elements, power electronic blocks are capable of working in two directions, when the grid works stably, the energy from the grid is stored in the storage element, when there is a sudden change in terms of voltage, energy from storage

elements will be brought back to overcome fluctuations and stabilize the grid, [2, 6, 9, 11, 13].

Grid system and consumption consumption: Electricity after production, through the converter is connected to the grid. From there the electrical loads are provided by the grid's electricity.

There are also measurement and control units with executive functions; Manage the operation of the entire grid system such as power generation control, power electronic converter control, grid connection control, and charge / discharge control of the energy storage system.

B. Storing electrical energy and stabilizing power source for energy balance

In the micro-grid: generators of diesel engines, hydroelectricity, renewable energy systems, etc., combine with power electronic converter to convert sinusoidal alternating voltage with frequency fit; connect directly to the national AC grid.The power generation systems all share the same grid frequency and these generators run at the same speed as ω_e. therefore we have equation (1), where $P_G = \Sigma P_{Gi}$, $P_L = \Sigma P_{Li}$ and $P_S = \Sigma P_{Gi}$. In equation (1) as well as all the kinetic equations of this paper, $p(.)$ is written as the derivative operator over time.

$$J_T p(\Delta\omega_e) = P_G - P_L - \Delta P_S \quad (1)$$

In the normal working state, the energy capacity comes from the solar power source; wind power; hydroelectric power, etc.., provide the grid enough to maintain a stable working state for the grid, but this capacity often changes continuously according to environmental conditions [2, 4, 7, 13].

Hence $\Delta P_S = 0$. Because $P_G = P_L$, $p(\Delta\omega_e) = 0$ has no variation in grid system frequency. The electric machines integrated in FESS then operate in motor mode and they store energy P_S is the capacity of the flywheel system system; P_G is the power pumped to the grid, for the grid to work stably, this capacity should always be kept constant with ($P_G = const$).

we have: $\Delta P_S \approx P_G - P_L$ (2)

Equation (2) shows the control of the grid frequency and the frequency of the renewable energies, in order to avoid the frequency difference of FESS from each other from the grid.

III. MODELING AND CONTROL OF THE ENERGY STORAGE FLYWHEEL

A. Principle of operation

Considering the system as shown in Fig. 1 with integrated energy storage flywheel, the block diagram of the energy storage flywheel system is shown in Figure 2, [4]. Under normal working conditions the electric machine in the flywheel works in motor mode, the flywheel performs energy storage in the form of kinetic energy. On the other hand, when there is an abnormal fluctuation in the power supply or the machine load in the flywheel acts as a generator providing the extra energy needed to keep the system stable. During energy discharge the speed of the flywheel decreases gradually resulting in constant voltage frequency change.

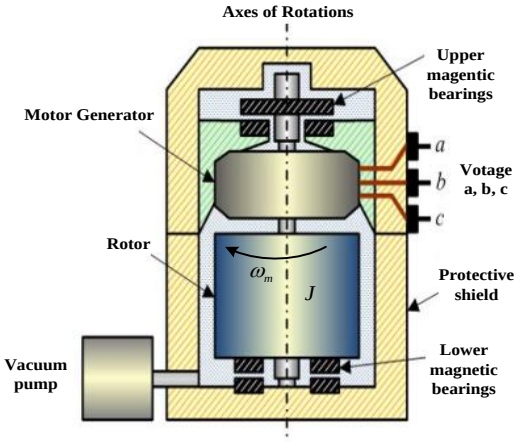

Fig 2: Structure diagram of flywheel system to store energy in microgrid, [4]

The stored energy density E_{vol} is given by (3) then $\sigma_r = \rho(l\omega_m)^2$ is the radial tensile stress applied to the flywheel. where ρ is the material density, ω_m the spinning angular speed and l the circular path radius of the considered elementary volume of FESS, [4, 5]. The coefficient K_F is related to the flywheel shape. By combining mass and volume density, the maximum storable energy is given by (4) where V is the flywheel volume and J its inertia.

$$E_{vol} = 0.5K_F\sigma_r \quad (3)$$

$$E_{k\,max} = 0.5J\omega_{R\,max}^2 \quad (4)$$

deduced $E_{k\,max} = 0.5K_F.V.\sigma_{r\,max}$ (5)

Related to the problem of charging and discharging the energy of the flywheel is given by equation (6):

$$J\frac{d\omega_m}{dt} = T_m - T_R \quad (6)$$

Inside T_m is the torque of the machine, T_R is the total friction moment; can be minimized through the use of a magnetic support (non-bearing design), [3, 8, 14].

B. Induction machine dynamic model

The induction machine is generally a squirrel cage induction machine thanks to the features of stable working; high reliability, low cost. For accurate control of torque (or power) of this machine, its dynamic equations are written in a synchronously rotating dq reference frame, and the corresponding model of this machine is shown clearly in [8], [9]. The basic voltage and flux components of this machine are given according to equations (7) and (8) respectively.

$$\begin{bmatrix}\psi_{sd}\\ \psi_{sq}\\ \psi_{rd}\\ \psi_{rq}\end{bmatrix}=\begin{bmatrix}L_s & 0 & L_m & 0\\ 0 & L_s & 0 & L_m\\ L_m & 0 & L_r & 0\\ 0 & L_m & 0 & L_r\end{bmatrix}\begin{bmatrix}i_{sd}\\ i_{sq}\\ i_{rd}\\ i_{rq}\end{bmatrix} \quad (7)$$

$$p.\begin{bmatrix}\psi_{sd}\\ \psi_{sq}\\ \psi_{rd}\\ \psi_{rq}\end{bmatrix}=-\begin{bmatrix}R_a & 0 & 0 & 0\\ 0 & R_a & 0 & 0\\ 0 & 0 & R_A & 0\\ 0 & 0 & 0 & R_A\end{bmatrix}\begin{bmatrix}i_{sd}\\ i_{sq}\\ i_{rd}\\ i_{rq}\end{bmatrix}+ \quad (8)$$

$$+\begin{bmatrix}0 & -\omega_s & 0 & 0\\ \omega_s & 0 & 0 & 0\\ 0 & 0 & -(\omega_s-\omega_m) & 0\\ 0 & (\omega_s-\omega_m) & 0 & 0\end{bmatrix}\begin{bmatrix}\psi_{sd}\\ \psi_{sq}\\ \psi_{rd}\\ \psi_{rq}\end{bmatrix}+\begin{bmatrix}v_{sd}\\ v_{sq}\\ 0\\ 0\end{bmatrix}$$

The components in the electric machine model are represented by the SI unit system. Inside: R_a and R_A are respectively the resistances of the stator windings and the rotor bars. $L_S = L_a + L_m$, $L_r = L_A + L_m$ and L_m are the stator, rotor and magnetizing inductances respectively. ω_S is the dq-frame rotating speed.

From $I_r = [i_{rd}\ i_{rq}]^T$, $\psi_s = [\psi_{sd}\ \psi_{sq}]^T$ and by taking the flux matrix in Equation (7) which is the representation of the flux components of the stator, the rotor current is calculated and given by Equation (9), where σ sums the components from the leakage flux.

$$\begin{bmatrix}i_{rd}\\ i_{rq}\end{bmatrix}=\frac{1}{L_r}\begin{bmatrix}\psi_{rd}\\ \psi_{rq}\end{bmatrix}-\frac{L_m}{L_r}\begin{bmatrix}i_{sd}\\ i_{sq}\end{bmatrix}=\sigma L_s\begin{bmatrix}i_{sd}\\ i_{sq}\end{bmatrix}+\frac{L_m}{L_r}\begin{bmatrix}\psi_{rd}\\ \psi_{rq}\end{bmatrix} \quad (9)$$

Inside, $$\sigma = 1-\frac{L_m^2}{L_s L_r} \quad (10)$$

Substituting expression (9) for expression (8) gives expression (11) as follows:

$$p\begin{bmatrix}i_{sd}\\ i_{sq}\\ \psi_{rd}\\ \psi_{rq}\end{bmatrix}=\begin{bmatrix}\frac{-1}{T_a} & \omega_s & \frac{1-\sigma}{\sigma L_m T_r} & \frac{(\sigma-1)\omega_m}{\sigma L_m}\\ -\omega_s & \frac{-1}{T_a} & \frac{(\sigma-1)\omega_m}{\sigma L_m} & \frac{1-\sigma}{\sigma L_m T_r}\\ \frac{L_m}{T_r} & 0 & \frac{-1}{T_r} & -g\omega_s\\ 0 & \frac{L_m}{T_r} & -g\omega_s & \frac{-1}{T_r}\end{bmatrix}\begin{bmatrix}i_{sd}\\ i_{sq}\\ \psi_{rd}\\ \psi_{rq}\end{bmatrix}+$$

$$+\frac{1}{\sigma L_S}\begin{bmatrix}1 & 0\\ 0 & 1\\ 0 & 0\\ 0 & 0\end{bmatrix}\begin{bmatrix}v_{sd}\\ v_{sq}\end{bmatrix} \quad (11)$$

Inside, $$T_a = \frac{\sigma T_S T_r}{T_r + (1-\sigma)T_S}; T_S = \frac{1}{R_a}; T_a = \frac{L_r}{R_A} \quad (12)$$

$$T_{em} = \frac{3n_p}{2}\frac{L_m}{L_r}(\psi_{rd} i_{sq} - \psi_{rq} i_{sd}) \quad (13)$$

The electromagnetic moment produced by an AC machine is given by equation (13). This torque component is generated from the speed of rotation of the flywheel written by Equation (6).

C. The energy converter model

The structure diagram of the converter is shown in figure 3. It consists of two bidirectional voltage sourced inverters (VSI) connected by a dc-link having a high-value filtering capacitor C_{dc}.

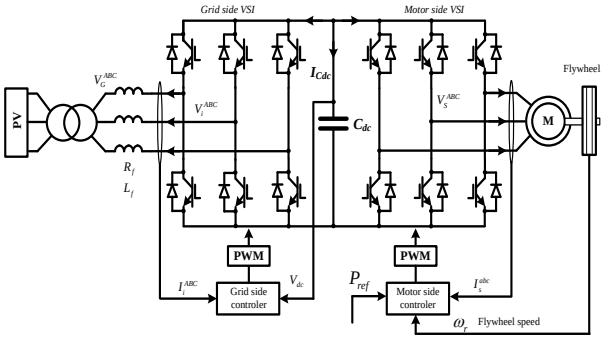

Fig 3: The back-to-back energy converter

From there, we design the controller model on the basis of the machine side (motor) and the microgrid side, with the VSI controller, by converting the coordinate system dq to DQ, according to [8 , 11]. The FESS side model is mainly driven by the ac torque of the ac machine as shown in Equation (6), such as the direct torque control (DTC) and the FOC control method, which are two common control problems. used for the VSI control model on the motor side, [2, 8]. The outstanding advantage of the FOC method is the separate control of the rotor flux component ψ_r and the electromagnetic torque T_m of the AC machine to achieve high efficiency, [3, 8]. According to (13) in the dq coordinate system, the component ψ_r is aligned with the d-axis, then $\psi_{rd} = \psi_r$ and $\psi_{rq} = 0$. From there we have:

$$T_m = K_\psi i_{sq};\ K_\psi = \frac{3n_p}{2}\frac{L_m}{L_r}\psi_r \quad (14)$$

$$\psi_r = \frac{L_m}{1+sT_r} i_{sd} \quad (15)$$

So we also have the current components i_{sd}, i_{sq} and voltage v_{sd}, v_{sq} as follows:

$$i_{sd} = \frac{K_a}{1+sT_a} v_{cd} \text{ and } i_{sq} = \frac{K_a}{1+sT_a} v_{cq} \quad (16)$$

Inside, $$K_a = \frac{T_a}{\sigma L_s} \quad (17)$$

$$v_{sd} = v_{cd} - \sigma L_s \omega_m i_{sq} \text{ and } v_{sq} = v_{cq} - \sigma L_s \omega_m i_{sd} \quad (18)$$

From (11) with the dq coordinate system and the corresponding phase angle component are written in (19):

$$\omega_s = \frac{L_m}{T_r \psi_r^{ref}} i_{sq} + \omega_m \text{ and } \theta_s = \int \omega_s dt \quad (19)$$

The energy stored in the flywheel is then given by equation (17) as follows:

$$E_K = \frac{J}{2}\omega_m^{*2} = \int P_{ref}\,dt \Rightarrow \omega_m^* = \sqrt{\frac{2}{J}\int P_{ref}\,dt} \quad (20)$$

From the grid side VSI output point of view figures.3 the whole microgrid is seen as a synchronous generator having L_f and R_f as stator leakage inductance and resistance. Then, the AC bus phase voltage is the derivative of a virtual grid flux ψ_G as given by (21). The grid side DQ-frame is attached to the space phasor of the grid's flux and the currents $I_i = \begin{bmatrix} i_{iD} & i_{iQ} \end{bmatrix}^T$ injected by the VSI is given by (22), (23). This equation is quite similar to the state equation of currents obtained forthe induction machine in (13). It comes that the two VSI control schemes are almost the same.

$$p(\psi_G^{ABC}) = V_G^{ABC} \quad (21)$$

$$p\begin{bmatrix} i_{iD} \\ i_{iQ} \end{bmatrix} = \begin{bmatrix} \frac{-1}{T_f} & \omega_e \\ -\omega_e & \frac{-1}{T_f} \end{bmatrix}\begin{bmatrix} i_{iD} \\ i_{iQ} \end{bmatrix} + \frac{1}{L_f}\begin{bmatrix} 0 & \omega_e \\ -\omega_e & 0 \end{bmatrix}\begin{bmatrix} \psi_{GD} \\ \psi_{GQ} \end{bmatrix} + \frac{1}{L_f}\begin{bmatrix} 0 & \omega_e \\ -\omega_e & 0 \end{bmatrix}\begin{bmatrix} v_{iD} \\ v_{iQ} \end{bmatrix} \quad (22)$$

Inside, $T_f = \frac{L_f}{R_f}$ (23)

The virtual flux ψ_G is orientated in the D-axis direction so that $\psi_G = \psi_D$ and $\psi_{GQ} = 0$, the instantaneous powers injected by the grid side VSI are given by (24). It follows that, the active power P_G can be controlled by i_{iQ} and the reactive power Q_G by i_D. The transfer functions of the injected currents are given by (25). The VSI reference voltages supplied to the PWM modulator are given by (26) and (27). The DQ transformation angle is obtained using the virtual flux calculator which formula is given by (28).

$$P_G = \frac{3\omega_e\psi_G}{sC_{cd}} i_{iQ};\; Q_G = \frac{3\omega_e\psi_G}{2} i_{iD} \quad (24)$$

$$i_{iD} = \frac{1/R_f}{1+sT_f} v_{cD};\; i_{iQ} = \frac{1/R_f}{1+sT_f} v_{cQ} \quad (25)$$

then: $v_{iD} = v_{cD} - L_f\omega_e i_{iQ}$ (26)

$$v_{iQ} = v_{cQ} - L_f\omega_e i_{iD} \quad (27)$$

$$\begin{bmatrix} \psi_{G\alpha} \\ \psi_{G\beta} \end{bmatrix} = \int\left(\begin{bmatrix} v_{i\alpha} \\ v_{i\beta} \end{bmatrix} - R_f\begin{bmatrix} i_{i\alpha} \\ i_{i\beta} \end{bmatrix}\right)dt - L_f\begin{bmatrix} i_{i\alpha} \\ i_{i\beta} \end{bmatrix} \quad (28)$$

$$\psi_G = \sqrt{\psi_{G\alpha}^2 + \psi_{G\beta}^2};\; \theta_G = tan^{-1}.\frac{\psi_{G\beta}}{\psi_{G_\alpha}} \quad (29)$$

The Q-axis reference current is provided by the dc-link voltage's control loop. The transfer function relating the Q-axis current and the dc voltage is given by (30). Then we have:

$$E_{dc} = \frac{-3\omega_e\psi_G}{sC_{dc}} i_{iQ};\; E_{dc} = V_{dc}^2 \quad (30)$$

The variable E_{dc} is a measure of the energy stored in the dc-link capacitor.

IV. THE SIMULATION AND EXPERIMENTATION

A. Simulation

After studying calculation, algorithm and modeling to control the energy storage flywheel system. The build the system on Matlab-Simulink with the following parameters, [14, 15]: Assuming that when there is a fluctuation in solar power capacity, the power system with integrated energy storage flywheel needs to pump one capacity into the micro-grid. 50kW, with:

$$P_f = P_g - P_{pv} = 50kW \quad (31)$$

In the normal working state, the photovoltaic battery capacity supplied to the grid is enough to maintain a stable working state of the micro-grid as $P_{pv} = P_g$. The electric machines integrated in the flywheel work in motor mode and electric charge 50kW of energy for 5 seconds, then discharge energy for the next 5 seconds to compensate for that energy shortage. The simulation parameters are as follows: Electric machine side: asynchronous machine integrated in flywheel P = 50kW, p = 2, R_s = 0,065Ω, R_r = 0,051Ω, L_s = 42,6.10^{-3}H, L_r = 42,5.10^{-3}H, M = 43.10^{-3}H, with the moment of inertia of the flywheel J_f = 160kgm^2. The initial speed of the flywheel: 1500 rpm, in accordance with (157 rad / s) and the reference power equal to the rated power of the machine (50kW). Grid side: three phase voltage, frequency 50Hz, the filter has: L_f = 11,5mH, R_f = 0,125Ω, C_{dc} = 15000μF, voltage in dc-link $V_{dc}^{ref} = 1200V$, working frequency PWM f_{PWM} = 5kH.

The simulation model on Matlab simulink of an ac machine with integrated flywheel to store energy is shown in Figure 4.

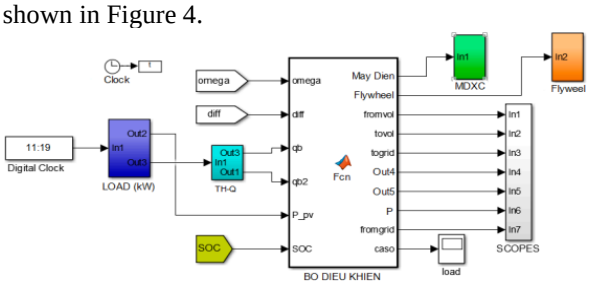

Fig 4: Schematic simulation system built on Matlab Simulink

Simulation time is 10 seconds, in which the first 5s of the flywheel are speed up from 1500 rpm to 3000 rpm then reduce the speed from 3000 rpm to 1500 rpm in the remaining time. The simulation results are shown in figures 5, 5, 6, 7.

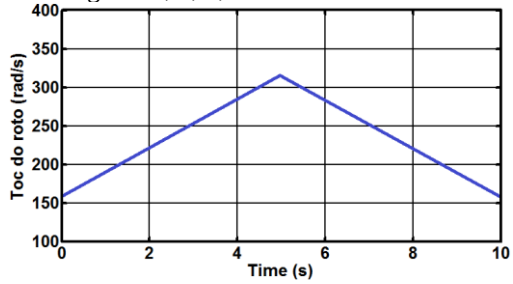

Fig 5: Speed of electric machine integrated in the flywheel

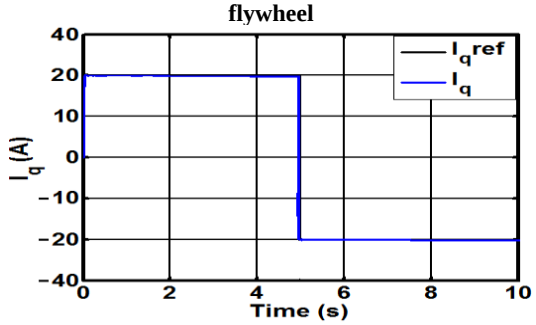

Fig 6: Component current curve i_q set and real current i_q

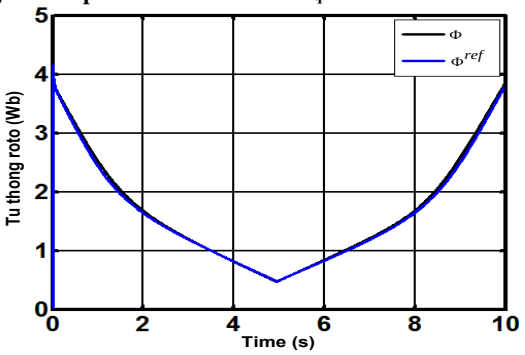

Fig 7: Curves of applied and net flux of machine connected to energy flywheel

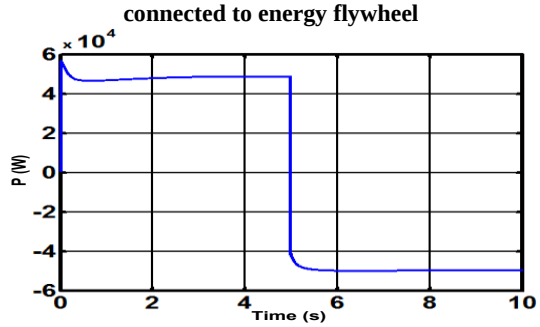

Fig 8: Transceiver capacity of the energy flywheel system

In which: Figure 6 shows the characteristic of machine speed integrated in the flywheel; Figure 6 shows the component curves iq of the applied current and actual current of the machine; Figure 7 shows the actual and applied flux curves of the machine connected to the flywheel; Figure 8 shows the transmit and receive power of the flywheel system.

Comment: Observing the above simulation results, we see that in a period of 0 to 5 seconds, the flywheel speed comes from the initial value of 1500 rpm, in accordance with (157 rad / s) is accelerated to 3000 rpm for 5 seconds. During this time the machine operates in the motor mode (positive power). In the remaining time, the flywheel speed is reduced from 3000 rpm to 1500 rpm, the machine works in generator mode (negative power), the energy stored in the flywheel in the form of kinetic energy. make compensation for wasted energy in the system.

B. Experiment

Experimental study with three-phase reverse flow system as shown in figure 9, including: Three phase AC motor, P = 2,2kW, U = 380V, I = 8,6A, speed 1500 rpm, p = 2, motor is hard coupled to the load: dc generator: P = 4kW, U = 220V, I = 8,6A, speed 1750 rpm, frequency 50Hz. Devices located on inverted table: current transformer 50A / 5A, power module IGBT 25A / 1200V, digital control module dsPIC30F4011, display module LCD-ICEA, oscilloscope, power source transformer, etc. The test system with inverters parameter table is as follows:

TABLE 1: Parameters to select devices for inverters

Description	Value
Rated power consume	10 kW
Voltage PV	60-150VDC
Voltage DC - link	700 V
Pulse frequency	10kHz
Filter cutoff frequency fc	25Hz
Capacitor C of the filter	4700 µF
Filter reactor L	2,5mH

Here we consider the independent voltage taken from the solar power system in the microgrid, put into the energy storage (battery, or energy storage flywheel) and then connected to the inverters. save, filter to supply power to the load side.

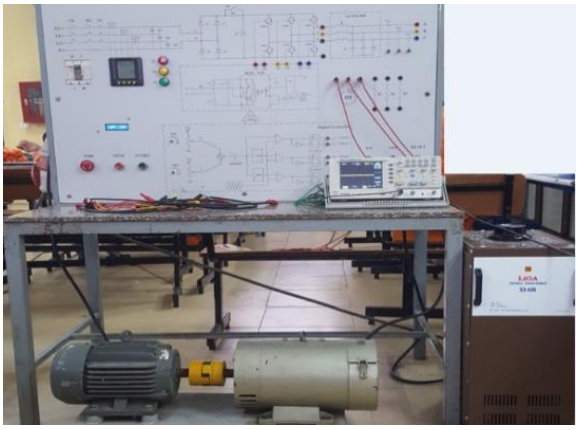

Fig 9: Image of experimental structure of three-phase inverse flow in the laboratory

The experimental model of the applied paper is the experimental results shown in Figure 10 and Figure 11.

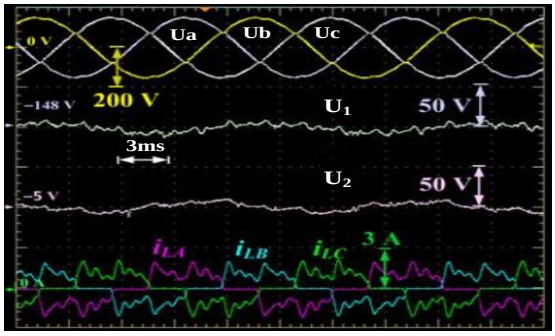

Fig 10: Three phase voltage response, phase current without filter

Stable load performance when changing 50% of voltage and current value. Without the converter and the filter, the value is then measured of the voltage on the load U_a; U_b; U_c is always sin wave (due to the quality of the inverter with digital controller module: Driver HCPL A3120; dsPIC 30F4011, etc.), value of current on load i_{LA}, i_{LB}, i_{LC}, changes significant (when frequency changes); Moreover, the values of voltage U_1, U_2 are two phase voltage values of the first phase and the second phase will be changed by 50%. Here the response time is from 0 to 30ms as shown in Figure 10.

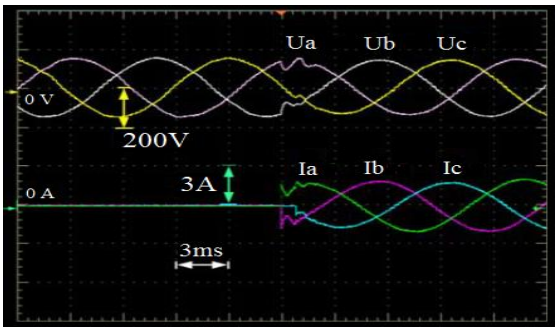

Fig 11: Voltage and current values of the system with variable load: from no load to load

The measured response is the voltage and current at the back of the inverter, when the filter is passed. At the time the system is operating with the load varies from no load to load, the change time is 15ms out of a total 30ms response time. Through research results, we can see that the system built has contributed to improving the quality of the renewable energy source for the micro-grid, which is always stable; bring about the standards of power quality, this is a new scientific issue, completely applicable to actual production, civil defense and security.

Comparing the results with studies in [4], and in previous studies [5, 6], the results of the paper are better than the simulation with time to reach small equilibrium value. in terms of current, voltage, and power values and having experimented with the system from obtained renewable energy sources, stored connected to a three phase reverse flow system, the load controller works well.

V. CONCLUSIONS

The improving the quality of renewable electrical energy in the micro-grid cannot use traditional storage technologies (batteries, batteries, micro-capacitors, etc.), but requires new technology to have many advantages than some of the previous energy storage technologies. The research results have shown the correctness and feasibility of the proposed solution. The system can be used to "smooth" and balance energy supply - demand in renewable energy systems that work independently or in connection with a microgrid. The results given in this paper are in accordance with the power quality standard IEEE 519.

ACKNOWLEDGMENT

This study was supported by University of Economics - Technology for Industries, Ha Noi - Vietnam; http://www.uneti.edu.vn/

REFERENCES

[1] Vo Minh Chinh, Pham Quoc Hai, Tran Trong Minh, "*Power electronics*", Science and Technics Publishing House, 2007.

[2] Tran Duc Chuyen, Tran Xuan Kien, "*Power electronics and application"*, Science and Technics Publishing House, 2017.

[3] Nguyen Doan Phuoc, "*Enhance control theory"*, Science and Technics Publishing House, 2009.

[4] Lai Khac Lai, Lai Thi Thanh Hoa, Nguyen Van Huynh, "*Fly wheel energy storage system in the microgrid with the renewable energy souces*", TNU Journal of Science and Technology, vol. 173, no. 12, pp. 587- 91, 2017.

[5] A.A. Khodadoost, Arani, H.Karami, G.B.Gharehpetian, M.S.A.Hejazi, "*Review of Flywheel Energy Storage Systems structures and applications in power systems and microgrids*", Renewable and Sustainable Energy Reviews, IEEE, pp 9-18, November, 2016.

[6] A. F. Tai-Ran Hsu, *"On a Flywheel-Based Regenerative Braking System for Regenerative Energy Recovery*", in Proceedings of Green and Systems Conference, Long Beach, 2013.

[7] Jacques Peronnet, *"Electrical Installation Guide: Calculations for Electricians and Designers*", According to IEC international standards; France, 2018.

[8] Nguyen Phung Quang, Jörg - Andreas Dittrich, *"Vector Control of Three - Phase AC Machines"*, Springer Science & Business Media, 2008.

[9] John Chiasson, *"Modeling and high performance control of electric machines"*, Wiley-IEEE Press. Published by Inc., Hoboken, New Jersey, Printed in the United States of America, 2005.

[10] Stuart Borlase, "*Smart grids Infrastructure, Technology, and Solutions*", Published by Taylor & Francis Group, LLC, 2013.

[11] S. Sumathi L. Ashok Kumar P. Surekha, Solar PV and Wind Energy Conversion Systems, Springer International Publishing AG Switzerland, 2016.

[12] Ahmed F Zobaa, Alfredo Vaccaro, "*Computational intelligence application in smart girds*", World Scientific Publishing Co. Pte. Ltd. 2015.

[13] J.C. Das, *"Power Systems Handbook Short-Circuits in AC and DC Systems"*, publishing International Standard Book New York, by Taylor & Francis Group, LLC, 2018.

[14] Andrea Bacciotti, *"Stability and Control of Linear Systems"*, Publishing Ltd; Springer Nature Switzerland AG 2019.

[15] László Keviczky, Ruth Bars, Jenő Hetthéssy, Csilla Bányász, Control Engineering: "*MATLAB Exercises*", Springer Nature Singapore Pte Ltd, USA ISSN 1439-2232, 2019.